J. Marine. Sci. Appl. (2011) 10: 429-436
DOI: 10.1007/s11804-011-1088-8

A Study on the Effect of Welding Sequence in Fabrication of Large Stiffened Plate Panels

Pankaj Biswas[1*], D. Anil Kumar[1], N. R. Mandal[2], and M. M. Mahapatra[3]

1. Department of Mechanical Engineering, IIT, Guwahati, India
2. Department of Ocean Engineering & Naval Architecture, IIT, Kharagpur, India
3. Department of Mechanical Engineering, IIT, Roorkee, India

Abstract: Welding sequence has a significant effect on distortion pattern of large orthogonally stiffened panels normally used in ships and offshore structures. These deformations adversely affect the subsequent fitup and alignment of the adjacent panels. It may also result in loss of structural integrity. These panels primarily suffer from angular and buckling distortions. The extent of distortion depends on several parameters such as welding speed, plate thickness, welding current, voltage, restraints applied to the job while welding, thermal history as well as sequence of welding. Numerical modeling of welding and experimental validation of the FE model has been carried out for estimation of thermal history and resulting distortions. In the present work an FE model has been developed for studying the effect of welding sequence on the distortion pattern and its magnitude in fabrication of orthogonally stiffened plate panels.
Keywords: elasto-plastic analysis; welding distortion; 3-D finite element analysis; stiffened panel; welding sequence
Article ID: 1671-9433(2011)04-429-08

1 Introduction

The temperature distributions due to welding play an important role in the resulting distortion of a welded structure. Most of the fusion welding processes are based on local heating of joining surfaces exceeding the melting temperature and then normal cooling to ambient temperature. The temperature distribution is highly non-uniform in nature. This non-uniform heating and cooling leads to incidence of residual stresses and structural deformation or distortion.

Over the years finite element methods have been used by many researchers to predict temperature distribution, residual stresses and distortion. Prominent among them are Friedman (1975), Michaleris and Debiccari (1997), Bonifaz (2000), and Tekriwal and Mazumdar (1988). Many researchers used the 2-D finite element analysis of Friedman to verify their 3-D computational modeling for the welding process.

Welding deformations are often calculated using analytical approaches (Rao, 1998; Watanbe and Satoh, 1961). Watanbe and Satoh (1961) used analytical methods resulting from the theory of elasticity for prediction of thermal deformations due to welding and line heating. However, since elastic solutions are limited, applications of the method are also limited.

Kamala and Goldak (1993) stated that 2-D approximation of a 3-D problem is not appropriate to predict temperature distribution, residual stresses and distortion patterns. Michaleris and DeBiccari (1997) combined two-dimensional welding simulations with three-dimensional structural analyses in a decoupled approach to evaluate welding induced buckling in panel structures. They had used a kinematic work hardening material model for simulating the plastic behavior of mild steel. Teng *et al.* (2001) used two-dimensional finite element analysis for predicting residual stresses and distortions in butt and fillet joints.

Depradeux and Jullien (2004) carried out thermomechanical analysis of the TIG process using temperature fields as input for subsequent structural analysis for predicting stress and displacements. Cheng (2005) investigated the effects of in-plane shrinkage strains on welding distortion in thin-wall structures based on three-dimensional axisymmetric modelling. Alberg (2005) developed modeling methodologies using finite element analysis for predicting deformation, residual stresses and material properties such as microstructure during and after welding as well as after heat treatment of fabricated aircraft-engine components.

Generally numerical thermal analysis is highly time consuming. To analyze a test sample with a size of 300mm ×300mm, 25.4mm thick in an SGI work station rated at 200MHz running under OS IRIX 6.2 requires about 12 695 seconds of CPU time (Yu *et al.,* 2001). To minimize computational time and cost axis-symmetry a modeling approach is adopted widely for welding simulation. Recent

Received date: 2011-05-10.
***Corresponding author Email:** pankaj.biswas@iitg.ernet.in

investigations have advocated a three-dimensional solid modeling without considering the axis-symmetry for better prediction of distortions and residual stresses (Kamala and Goldak, 1993). Works related to three dimensional finite element analysis without considering the half-symmetry for predicting angular distortions are rarely found in research literature. Fanous *et al.* used element birth and element movement techniques for three-dimensional axis-symmetric modeling of butt joints.

In this work both finite element methods were used for a simple case of butt welding. To simulate the filler material deposition, the 'Element Birth' (Fanous *et al.*, 2003) approach has been used in the numerical model. In this technique the elements are activated or deactivated as the welding heat source moves along the weld line. The temperature distribution patterns were first obtained followed by residual distortions caused by welding.

After verification of the 3-D FE model (Biswas *et al.*, 2006; Biswas *et al.*, 2007; Biswas *et al.*, 2008) the same methodology has been applied to study the distortion behavior of large stiffened panels. Here an FE model has been applied for studying the effect of welding sequence on the distortion pattern and its magnitude in fabrication of orthogonally large stiffened plate panels. The model and the methodology developed in the present work for predicting the effect of welding sequences in residual distortion of orthogonally large stiffened plate panels compared fairly well with experimental results. The model and the methodology developed in the present work can be utilized for choosing the right welding sequence which will yield minimum residual distortion for fabrications of orthogonally large stiffened plate panels.

2 Thermal modeling

A three dimensional finite element thermal model was used in the present work to analyze the heat transfer and temperature distribution in SMA welding. From a literature survey it is clear that the heat transfer mechanism in a molten pool is extremely complex. The various material properties of the metals in the molten state are also not authentically established. In arc welding, except for a small volume of metal, most of the portion of the work piece remain in a solid state. Therefore a three dimensional conduction model was considered to analyze the heat flow and the resulting temperature distribution over the entire plate.

The governing differential equation for heat conduction for a homogenous, isotropic solid without heat generation in the rectangular coordinate system (x, y, z) can be expressed as:

$$\frac{\partial}{\partial x}\left(K\frac{\partial T}{\partial x}\right)+\frac{\partial}{\partial y}\left(K\frac{\partial T}{\partial y}\right)+\frac{\partial}{\partial z}\left(K\frac{\partial T}{\partial z}\right)=\rho c\frac{\partial T}{\partial t} \quad (1)$$

where, K= thermal conductivity, T=temperature, ρ= density of the material, c = specific heat and t = time.

Eq.(1) can be written as:

$$\rho c\frac{\partial T}{\partial t}=-\boldsymbol{L}^{\mathrm{T}}\boldsymbol{q} \quad (2)$$

where

$\boldsymbol{L}=\begin{Bmatrix}\frac{\partial}{\partial x}\\ \frac{\partial}{\partial y}\\ \frac{\partial}{\partial z}\end{Bmatrix}$ is vector operator and $\boldsymbol{q}$ is heat flux vector.

$$\boldsymbol{L}^{\mathrm{T}}\boldsymbol{q}=\nabla\boldsymbol{q} \quad \text{and} \quad \boldsymbol{L}T=\nabla T$$

where, ∇ represents grad operator.

Fourier's law is used to relate the heat flux vector to the thermal gradient

$$\boldsymbol{q}=-\boldsymbol{D}\boldsymbol{L}T$$

where, $\boldsymbol{D}=\begin{bmatrix}K & 0 & 0\\ 0 & K & 0\\ 0 & 0 & K\end{bmatrix}$ is conductivity matrix.

Eq.(2) can be written as:

$$\rho c\frac{\partial T}{\partial t}=\boldsymbol{L}^{\mathrm{T}}\left(\boldsymbol{D}\boldsymbol{L}T\right) \quad (3)$$

To solve Eq.(3), a set of boundary conditions is needed.

(i) Initial condition

A specified initial temperature for the welding that covers all the elements of the specimen:

$$T=T_{\infty} \quad \text{for } t=0 \quad (4)$$

where T_{∞} is the ambient temperature.

To develop first and second boundary conditions the energy balance has been considered at the work surface as:

Heat supply = Heat loss.

(ii) First boundary condition

A specific heat flows acting over surface of welding region.

$$q_n=-q_{\mathrm{sup}} \quad (5)$$

The quantity q_n represents the component of the conduction heat flux vector normal to the work surface. The quantity q_{sup} represents the heat flux supplied to the work surface in $\frac{W}{m^2}$, from an external welding arc.

$$q_n=\boldsymbol{q}^{\mathrm{T}}\boldsymbol{n} \quad \text{on the surface weld region for } t>0 \quad (6)$$

where, $\boldsymbol{n}$ is unit outward normal vector.

(iii) Second boundary condition

Considering heat loss (q_{conv}) due to convection over the whole surface of a stiffened plate panel (Newton's law of

cooling):

$$q_n = q_{\text{conv}} \quad \text{or} \quad \boldsymbol{q}^{\mathrm{T}}\boldsymbol{n} = h_f\left(T - T_\infty\right) \quad \text{for} \quad t > 0 \tag{7}$$

Pre-multiplying Eq.(3) by a virtual change in temperature, integrating over the volume of the element, combining with Eqs.(6) and (7), and with some algebraic manipulation we get:

$$\begin{aligned}&\int_{\text{vol}}\left(\rho c\delta T\left(\frac{\partial T}{\partial t}\right)+\boldsymbol{L}^{\mathrm{T}}\left(\delta T\right)\left(\boldsymbol{DLT}\right)\right)\mathrm{d}\left(\text{vol}\right)=\\&\int_{S_1}\delta T q_{\text{sup}}\mathrm{d}S_1+\int_{S_1+S_2}\delta T h_f\left(T_\infty-T\right)\mathrm{d}\left(S_1+S_2\right)\end{aligned} \tag{8}$$

where, vol = volume of the element; δT = an allowable virtual temperature $\left(=\delta T\left(x,y,z,t\right)\right)$.

2.1 Derivation of heat flow matrices

The variable T is allowed to vary both in space and time. This dependency is expressed as shown in Eq.(2.9).

$$T = \boldsymbol{N}^{\mathrm{T}}\left\{T_e\right\} \tag{9}$$

where, $T = T\left(x,y,z,t\right)$ is temperature, $\boldsymbol{N} = \boldsymbol{N}\left(x,y,z\right)$ is element shape function and $\boldsymbol{T}_e = \boldsymbol{T}_e\left(t\right)$ is nodal temperature vector.

The time derivative of Eq.(2.9) may be written as shown in Eq.(2.10).

$$\dot{T} = \frac{\partial T}{\partial t} = \boldsymbol{N}^{\mathrm{T}}\left\{\dot{T}_e\right\} \tag{10}$$

δT has the same form as T as shown in Eq.(11).

$$\delta T = \boldsymbol{\delta T}_e^{\mathrm{T}}\boldsymbol{N} \tag{11}$$

The combination of $\boldsymbol{L}T$ is written as shown in Eq.(12).

$$\boldsymbol{L}T = \boldsymbol{B}\boldsymbol{T}_e \tag{12}$$

where, $\boldsymbol{B} = \boldsymbol{L}\boldsymbol{N}^{\mathrm{T}}$

Now the variational statement of Eq.(8) can be combined with Eqs.(9, 10, 11 & 12) to yield Eq.(13).

$$\begin{aligned}&\int_{\text{vol}}\rho\, c\,\boldsymbol{\delta T}_e^{\mathrm{T}}\boldsymbol{N}\boldsymbol{N}^{\mathrm{T}}\dot{\boldsymbol{T}}_e\,\mathrm{d}\left(\text{vol}\right)+\int_{\text{vol}}\boldsymbol{\delta T}_e^{\mathrm{T}}\boldsymbol{B}^{\mathrm{T}}\boldsymbol{D}\boldsymbol{B}\boldsymbol{T}_e\,\mathrm{d}\left(\text{vol}\right)=\\&\int_{S_1}\boldsymbol{\delta T}_e^{\mathrm{T}}\boldsymbol{N}\,q_{\text{sup}}\,\mathrm{d}S_1+\int_{S_2}\boldsymbol{\delta T}_e^{\mathrm{T}}\boldsymbol{N}h_f\left(T_\infty-\boldsymbol{N}^{\mathrm{T}}\boldsymbol{T}_e\right)\mathrm{d}S_2\end{aligned} \tag{13}$$

In this present situation the density ρ is assumed to remain constant and specific heat c may vary over the element. Finally $\boldsymbol{T}_e, \dot{\boldsymbol{T}}_e$ and $\boldsymbol{\delta T}_e$ are nodal quantities and do not vary over the element, so that they can be taken out from the integrals. Now, since all quantities are pre-multiplied by $\boldsymbol{\delta T}_e$, this term may also be dropped from the resulting equation. Thus Eq.(13) is reduced to Eq.(14).

$$\begin{aligned}&\rho\int_{\text{vol}}c\,\boldsymbol{N}\boldsymbol{N}^{\mathrm{T}}\mathrm{d}\left(\text{vol}\right)\dot{\boldsymbol{T}}_e+\int_{\text{vol}}\boldsymbol{B}^{\mathrm{T}}\boldsymbol{D}\boldsymbol{B}\,\mathrm{d}\left(\text{vol}\right)\boldsymbol{T}_e=\\&\int_{S_1}\boldsymbol{N}\,q_{\text{sup}}\mathrm{d}S_1+\int_{S_2}T_\infty\boldsymbol{N}\,h_f\,\mathrm{d}S_2-\int_{S_2}h_f\boldsymbol{N}\boldsymbol{N}^{\mathrm{T}}\boldsymbol{T}_e\,\mathrm{d}S_2\end{aligned} \tag{14}$$

Eq.(14) can be rewritten as shown in Eq.(2.15).

$$\boldsymbol{C}_e^{\,t}\dot{\boldsymbol{T}}_e+\left(\boldsymbol{K}_e^{\,th}+\boldsymbol{K}_e^{\,tc}\right)\boldsymbol{T}_e=\boldsymbol{Q}_e^{\,f}+\boldsymbol{Q}_e^{\,c} \tag{15}$$

where,

$\boldsymbol{C}_e^{\,t}=\rho\int_{\text{vol}}c\boldsymbol{N}\boldsymbol{N}^{\mathrm{T}}\mathrm{d}\left(\text{vol}\right)$ is element specific heat matrix,

$\boldsymbol{K}_e^{\,th}=\int_{\text{vol}}\boldsymbol{B}^{\mathrm{T}}\boldsymbol{D}\boldsymbol{B}\mathrm{d}\left(\text{vol}\right)$ is element diffusion conductivity matrix,

$\boldsymbol{K}_e^{\,tc}=\int_{S_2}h_f\boldsymbol{N}\boldsymbol{N}^{\mathrm{T}}\mathrm{d}S_2$ is element convection surface conductivity matrix,

$\boldsymbol{Q}_e^{\,f}=\int_{S_1}\boldsymbol{N}q_{\text{sup}}\mathrm{d}S_1$ is element heat flow vector for surface S_1 and

$\boldsymbol{Q}_e^{\,c}=\int_{S_2}T_\infty h_f\boldsymbol{N}\,\mathrm{d}S_2$ is element convection for surface S_2 heat flow vector.

2.2 Assumptions made in the thermal model

In developing the thermal model, an attempt was made to accommodate the actual welding conditions as much as possible. However the following factors have been assumed in the formulation of the thermal model of the welding process.

1) All the relevant properties of steel except density were considered as a function of temperature.

2) Linear Newtonian convection cooling was considered on all the surfaces excepting the weld zone.

3) Heat flux was considered as an applied load along the weld line.

4) During welding, the work piece receives energy both from the arc as well as from the metal droplets. The arc energy remains fairly constant and does not change significantly with time whereas the energy transfer from the metal droplets depends on various parameters such as the metal transfer mode, frequency of droplets, droplet size and its temperature. Now these phenomena are very much transient in nature and the resulting complexity makes them extremely difficult to incorporate in a numerical scheme. Therefore, the total energy transfer from arc and metal droplets have been coupled together and expressed as an overall arc heat transfer efficiency. Arc efficiency (= 0.75) (Okada, 1977) was taken into account for other losses.

2.3 Thermo-mechanical analysis

For evaluating the distortion, the heat transfer analysis was carried out first to find out the nodal temperatures as a function of time. Then in the second part of the analysis the thermo-mechanical nonlinear elasto-plastic analysis was done from the result obtained from the heat transfer analysis. Von Mises yield criterion and associated flow rules (Cheng, 2005; Alberg, 2005) were considered in the modeling. In the structural analysis boundary conditions which prevented rigid body motions were also imposed into the modeling. In the present work eight nodded brick elements were used for

the thermal analysis and eight similar nodded elements were used in the structural analysis. The details of thermo-mechanical analysis were presented in our previous published study (Biswas and Mandal, 2008). Fig.1 shows the flow chart of FEM mechanical analysis for prediction of residual deformations due to the welding process.

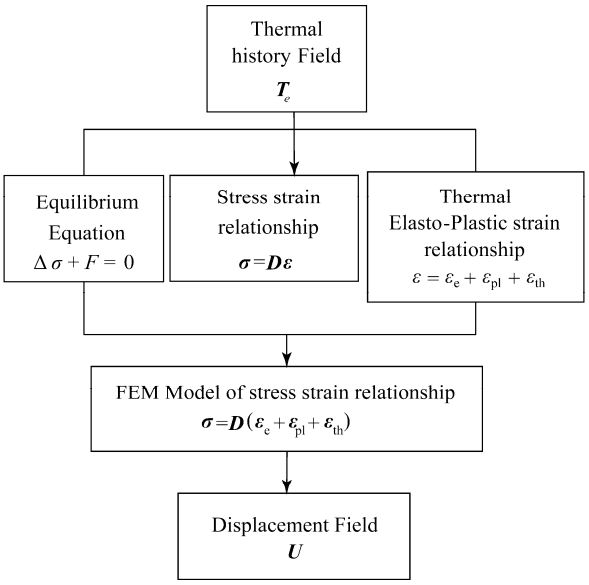

Fig.1 Flow chart of FEM mechanical analysis for predicting of weld induced distortion

where, $\boldsymbol{\sigma}$ is stress vector, $\boldsymbol{D}$ is stiffness matrix, ε is total strain,ε_e is elastic strain, ε_{pl} is plastic strain and ε_{th} is thermal strain.

3 Material properties

In the present analysis, the material properties of C-Mn steel were used as given by Brown and Song (1992). Table 1 shows the temperature dependent material properties used for the transient heat transfer and elasto-plastic analysis. Temperature dependent convection coefficients (Adak and Mandal, 2003) for steel surfaces are given in Table 2.

Table 1 Temperature dependent material properties of C-Mn steel

Temp /°C	Thermal conductivity /(W·m^{-1} °K)	Specific heat /(J/kg °K)	Thermal expansion co-efficient /(10^{-6}/°C)	Young modulus /GPa	Poisson ratio
0	51.9	450	10	200	0.2786
100	51.1	499.2	11	200	0.3095
300	46.1	565.5	12	200	0.331
450	41.05	630.5	13	150	0.338
550	37.5	705.5	14	110	0.3575
600	35.6	773.3	14	88	0.3738
720	30.64	1080.4	14	20	0.3738
800	26	931	14	20	0.4238
1450	29.45	437.93	15	2	0.4738
1510	29.7	400	15	0.2	0.499
1580	29.7	735.25	15	0.00002	0.499
5000	42.2	400	15.5	0.00002	0.499

Table 2 Temperature dependent convection coefficients for steel surfaces

Temperature /°K)	Convection Coefficient /(W·m^{-2} K)
78	9.079
556	18.15
2778	52.66
3778	1089

Table 3 Temperature dependent yield stress for steel

Temp. /°K	293	373	573	773	973	1073	1273	1473	1673
Yield stress (σ_y) /MPa	398	379	305	192	41	36	28	20	12

Table 4 Temperature dependent enthalpy for steel

Temperature /°C	Enthalpy /(MJ·m^{-3})	Temperature /°C	Enthalpy /(MJ·m^{-3})
0	0	600	2500
100	360	700	3000
200	720	800	3700
300	1100	900	4500
400	1500	1000	5000
500	1980	>2500	9000

4 Effect of welding sequence in welded structures

A three dimensional finite element modeling strategy was developed to study the effect of welding sequence of large stiffened plate panels. It was observed form the distortion pattern of the welded structure that the sequence from welding of stiffeners has a significant effect on structural distortion. The welding parameters used in the present investigation are shown in Table 5.

Table 5 Welding parameters used in numerical analysis

Current / A	Voltage / V	Welding speed / (mm·s^{-1})
60	27	2.0

The dimensions of the panels are such that it is virtually impossible to carry out transient thermo-elasto-plastic analysis to estimate weld induced distortions. The stiffened panels consisted of a 6mm thick 2000 mm×800 mm C-Mn steel plate with 2 longitudinal stiffeners (50 mm×50 mm× 5mm) and 2 transverse stiffeners (100 mm×100 mm×10 mm). Thus a situation of an orthogonally stiffened panel as used in ship structure was created. However, transient thermo-elasto-plastic analysis of such a structure using Pentium IV, 2.66 GHz computer with 3.0 GB RAM proved to be impossible using the conventional finite element approach. For making the problem tangible to FE transient analysis, the quasi-stationary nature of welding process and the resulting symmetric behavior of the stiffened panel has been effectively used. The FE model and meshing view of a part of the panel along with stiffener is shown in Fig.2. The CPU time needed to analyze the model shown in Fig.3 was

about 4½ to 5 hours.

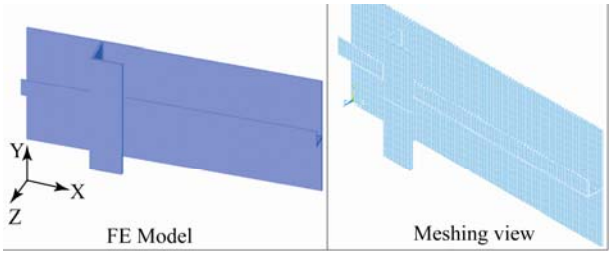

Fig.2 Finite element model and meshing view of a part of the plate panel

Two different sequences of welding of stiffeners as shown in Figs.3 and 4 were examined. The spacing between the transverse members and longitudinal members are shown in Fig.4. From the results as shown in Figs.5 and 6 one can observe that the extent of deformation tends to reduce with a specific pattern of welding sequence. From FE analysis it was seen that welding sequences have a significant effect on weld induced distortion patterns. From this study it was seen that the weld induced distortion is much less in case-2 compared to case-1 welding sequences. The weld induced distortion patterns obtained from FE analysis were verified with experimental results as described in section 5.

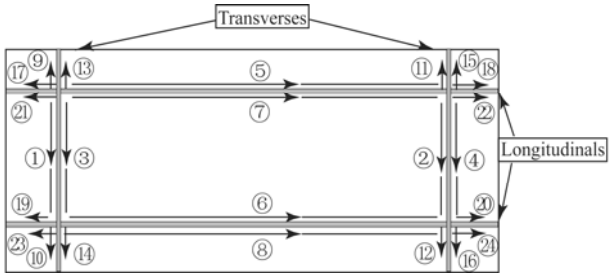

Fig.3 Welding sequences for case 1

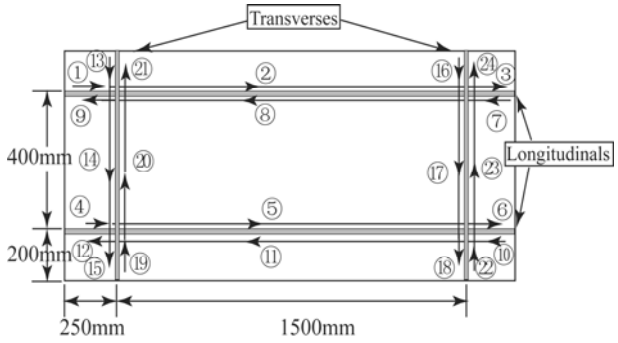

Fig.4 Welding sequences for case 2

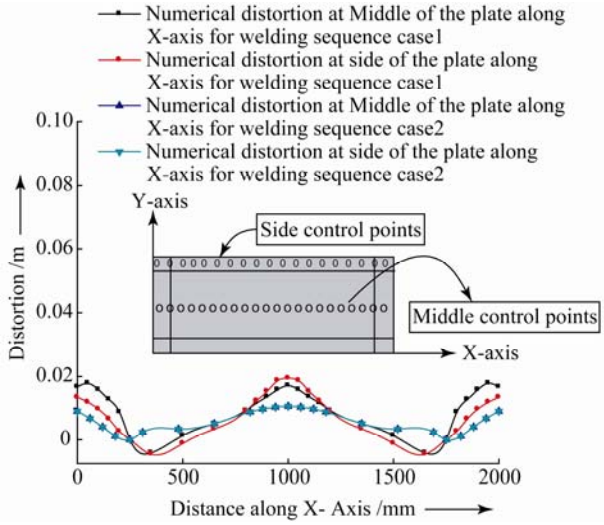

Fig.5 Comparison of numerical distortion along X-axis at the side and mid plane of the plate for welding sequence case1 and case2

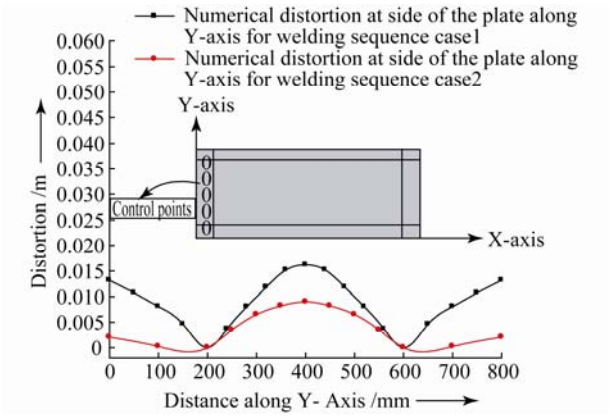

Fig.6 Comparison of numerical distortion along Y-axis at the side and mid plane of the plate for welding sequence case1 and case2

5 Experimental results

Before welding, the stiffeners were tack welded to the base plate. Then initial measurements of the plate top surface at the predefined locations were taken with respect to a fixed datum by using a linear variable differential transducer (LVDT) as shown in Fig.7. The LVDT was mounted on a suitable carriage which had three degrees of motion. Subsequent welding was carried out using shielded metal arc welding. After the plate cooled down to an ambient temperature, plate surface measurements were taken at the previously mentioned locations using an LVDT. The difference between the measurements before and after welding gave the actual distortion of the welded plate.

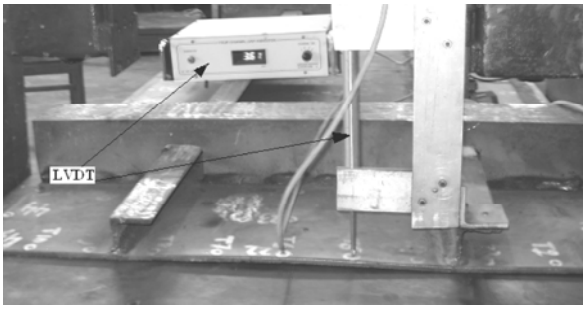

Fig. 7 Distortion measurement setup using LVDT

5.1 Comparison between numerical and experimental results

Experimentally measured welding parameters used for analysis are shown in Table 6. The dimension, coordinate system (x, y, z) and control points for measuring residual distortion are shown in Fig. 8. Post welding deformations of plates are shown in Figs. 9 and 10.

Table 6 Experimental welding parameters

Current / A	Voltage / V	Welding speed /(mm·s^{-1})
160	27	2.0

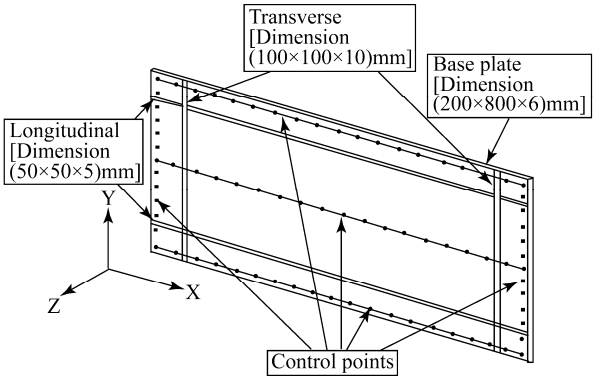

Fig. 8 Control points for measurement of distortions

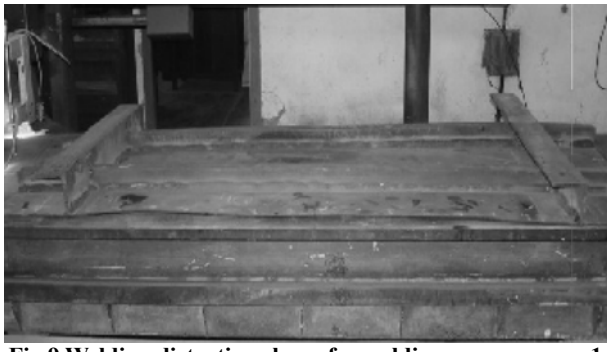

Fig.9 Welding distortion shape for welding sequence case1

Fig.10 Welding distortion shape for welding sequence case2

Comparison of numerical and experimental distortion of the full scale stiffened panel at the plate edge and the mid plane of the plate are shown in Figs.11 and 12 respectively.

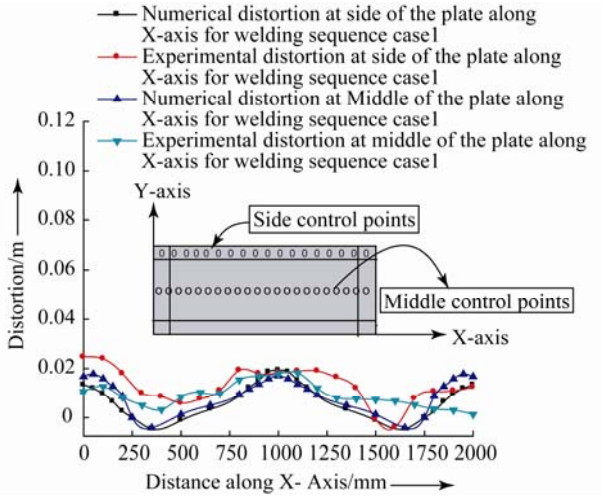

Fig.11 Comparison of numerical and experimental distortion at the side and mid plane of the plate for welding sequence case1

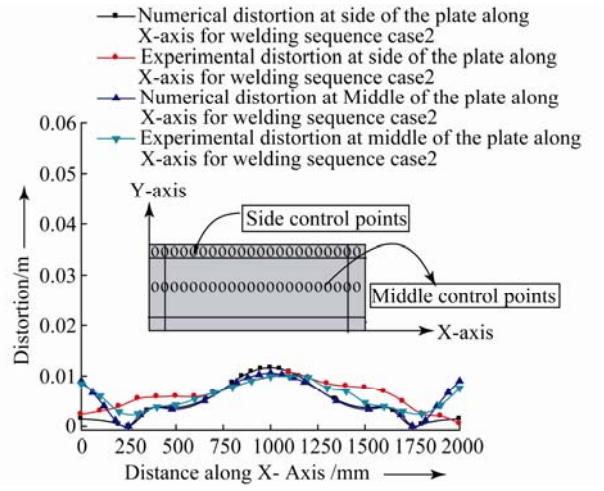

Fig.12 Comparison of numerical and experimental distortion at the side and mid plane of the plate for welding sequence case2

From Figs.11 and 12, one can observe that the sequence of welding stiffeners as depicted in Fig.4 led to minimum residual deformation of the entire stiffened panel. Hence

this welding sequence if followed in real life structures will result in stiffened panels with minimum deformation.

6 Conclusions

The effect of the welding sequence on the resulting deformation of a large stiffened panel was studied for two different cases. The following conclusions can be derived from the present investigation:

1) It was observed that the welding sequence on the stiffened panel has a significant effect on resulting distortion.

2) A feasible three-dimensional finite element model for predicting distortions due to different welding sequences of large stiffened plate panels have been developed utilizing the quasi-stationary nature of the welding process and the symmetric behavior of the stiffened panels.

3) The distortions obtained through analysis and those obtained from experimental measurements compared fairly well with a variation of about only 5 to 15 percent.

4) The trends and patterns of resulting distortion for orthogonally stiffened panels could be established fairly easily by this model. The benefit of the same can be implemented in a shipyard environment without much difficulty.

References

Adak M, Mandal NR (2003). Thermo-mechanical analysis through a Pseudo- linear equivalent constant stiffness system. *Journal of Engineering for the Maritime Environment*, **217**(M1), 1-9.

Alberg H (2005). Simulation of welding and heat treatment modelling and validation. PhD thesis, Lulea University of Technology, Sweden.

Biswas P, Mandal NR, Sha OP (2006). Numerical and ANN prediction of thermal history of submerged arc welding. *Journal of Mechanical Behavior of Materials*, **17**(4), 269-286.

Biswas P, Mandal NR, Sha OP (2007). Prediction of process parameters of line heating process by three dimensional finite element method. *Proc.IMechE, J. Engineering for the Maritime Environment*, **221**(Part M), 17-30.

Biswas P, Mandal NR (2008). Welding distortion simulation of large stiffened plate panels. *Journal of Ship Production*, **24**(1), 50-56.

Bonifaz E (2000). Finite element analysis of heat flow in single-pass arc welds. *Welding Research Supplements*, May, 121-125.

Brown S, Song H (1992). Implication of three-dimensional numerical simulations of welding large structures. *Weld. J.*, **71**(2), 55s-62s.

Cheng W (2005). In-plane shrinkage strains and their effects on welding distortion in thin-wall structures. PhD thesis, The Ohio State University, USA.

Depradeux L, Jullien JF (2004). Experimental and numerical simulation of thermomechanical phenomena during a TIG welding process. *J. Physic. IV France*, **120**, 697-704.

Fanous FZ. Ihab, Younan Maher YA, Wifi, S A (2003). 3-D Finite element modelling of the welding process using element birth and element movement techniques. *Tran. ASME, J. Pressure Vessel Technol.*, **125**, 144-150.

Friedman E (1975). Thermo mechanical analysis of the welding process using the finite element method. Transaction of ASME, 206-213.

Kamala V, Goldak J. A (1993). Error due to two dimensional approximation in heat transfer analysis of welds. *Weld. J.*, **72**(9), 440s-446s.

Mandal NR, Adak M (2001). Fusion zone and HAZ prediction through 3-D simulation of welding thermal cycle. *Journal of the Mechanical Behavior of Materials*, **12**(6), 401-414.

Michaleris P, Debiccari A (1997). Prediction of welding distortion. *Welding Journal*, April, 172-180.

Okada A (1977). Application of melting efficiency and its problems. *Journal of Japan Welding Society*, **46**, 53-61.

Rao PN (1998). *Manufacturing technology*. Tata McGraw-Hill Pub. Co. Ltd., New Delhi.

Teng TL, Fung CP, Chang PH, Yang WC (2001). Analysis of residual stresses and distortions in T-joint fillet welds. *International Journal of Pressure Vessels and Piping*, **78**, 523-538.

Tekriwal P, Mazumdar J (1988). Finite element analysis of three dimensional heat transfer in gas manual arc welding. *Welding Research Supplement, Welding Journal*, July, 150-156.

Watanbe M, Satoh K (1961). Effect of welding conditions on the shrinkage and distortion in welded structures. *Weld. J.*, **40**(8), 377s-384s.

Yu G, Anderson RJ, Maekawa T, Patrikalakis NM (2001). Efficient simulation of shell forming by line heating. J*ournal of Mechanical Sciences*, **43**, 2349-2370.

List of symbols:

x,y,z	coordinate
h_f	convection heat transfer coefficient (W/m^2 K)
q_n	component of conduction heat flux normal to the work surface (W/m^2)
k	thermal conductivity (W/m K)
c	specific heat (J/kg K)
η	heat efficiency of the arc
q_{sup}	supplied heat flux from the welding arc (W/m^2)
q_{conv}	heat loss from the work surfaces by convection (W/m^2)
r	radial distance in the welding arc (mm)
S_1	welding surface where heat flux applied
S_2	surface where convection applied
t	time (sec)
V	welding voltage (volt)
Q	arc power (W)
T	temperature (^{0}C)
T_∞	the surroundings temperature (^{0}C)
∇	differential operator
ε_e	the elastic strain
ε	total strain
ε_{pl}	plastic strain
ε_{th}	thermal strain
σ	the stress
$\boldsymbol{\sigma}$	stress vector
$\boldsymbol{D}$	stiffness matrix
ρ	density of the base metal (kg/m^3)

Dr. Pankaj Biswas was born in 1979. He is an Assistant Professor of IIT Guwahati, Dept. of Mechanical Eng. His current research interests include manufacturing and design: computational weld mechanics, ship production, line heating, and FE structural analysis.

Mr. D. Anil Kumar was born in 1983. He is a Research Scholar of IIT Guwahati, Dept. of Mechanical Eng. His current research interests include manufacturing: computational weld mechanics and FE thermo mechanical analysis.

Dr. Nisith Ranjan Mandal was born in 1954. He is a professor of IIT Kharagpur, Dept. of OE&NA. His current research interests include ship production, ship design, line heating, welding distortion of large stiffened structures and welding techniques.

Dr. M. M. Mahapatra was born in 1970. He is working as an assistant professor in the Mechanical and Industrial Engineering Department at Indian Institute of Technology, Roorkee. His current research interests include plate forming by line heating, welding deformation, welding residual stress analysis, and design of welded structures.

.
